The Cryosphere Discuss., 5, 1583–1625, 2011
www.the-cryosphere-discuss.net/5/1583/2011/
doi:10.5194/tcd-5-1583-2011


The Cryosphere Discussions



# Comparison of MODIS-derived land surface temperatures with near-surface soil and air temperature measurements in continuous permafrost terrain

**S. Hachem**[1], **C. R. Duguay**[1], **and M. Allard**[2]

[1]Interdisciplinary Centre on Climate Change and Department of Geography and Environmental Management, University of Waterloo, Waterloo, Ontario N2L 3G1, Canada
[2]Centre d'études nordiques and Département de Géographie, Université Laval, Québec, Québec G1K 7P4, Canada

Received: 29 April 2011 – Accepted: 4 May 2011 – Published: 27 May 2011

Correspondence to: S. Hachem (hachem_sonia@yahoo.fr)

Published by Copernicus Publications on behalf of the European Geosciences Union.







## Abstract

In Arctic and sub-Arctic regions, meteorological stations are scattered and poorly distributed geographically; they are mostly located along coastal areas and are often unreachable by road. Given that high-latitude regions are the ones most significantly affected by recent climate warming, there is a need to supplement existing meteorological station networks with spatially continuous measurements such as those obtained by spaceborne platforms. In particular, land surface (skin) temperature (LST) retrieved from satellite sensors offer the opportunity to utilize remote sensing technology to obtain a consistent coverage of a key parameter for climate, permafrost, and hydrological research. The Moderate Resolution Imaging Spectroradiometer (MODIS) sensor aboard the Terra and Aqua satellite platforms offers the potential to provide spatial estimates of near-surface temperature values. In this study, LST values from MODIS were compared to ground-based near-surface air and soil temperature measurements obtained at herbaceous and shrub tundra sites located in the continuous permafrost zone of northern Québec, Canada, and the North Slope of Alaska, USA. LST values were found to be better correlated with near-surface air temperature (1–2 m above the ground) than with soil temperature (3–5 cm below the ground) measurements. A comparison between mean daily air temperature from ground-based station measurements and mean daily MODIS LST, calculated from daytime and nighttime temperature values of both Terra and Aqua acquisitions, for all sites and all seasons pooled together reveals a high correlation between the two sets of measurements ($R > 0.93$ and mean difference of −1.86 °C). Mean differences ranged between −0.51 °C and −5.13 °C due to the influence of surface heterogeneity within the MODIS 1 km$^2$ grid cells at some sites. Overall, it is concluded that MODIS offers a great potential for monitoring surface temperature changes in high-latitude tundra regions and provides a promising source of input data for integration into spatially-distributed permafrost models.





TCD
5, 1583–1625, 2011



## 1 Introduction

The 2007 Intergovernmental Panel on Climate Change (IPCC) reports a global temperature increase of 0.74 °C over the last 100 years. Observational records show that average temperature in the Arctic has risen at almost twice the rate as the rest of the world in the past few decades (Zhou et al., 2001; Hinzman et al., 2005). Near-surface air temperature trends in the Arctic have been shown to be greater for inland regions than coastal/ocean regions (Comiso, 2003). There are clear signs that change is ongoing in other environmental variables as well. In addition to air temperature, annual precipitation are increasing in many regions; spring snow cover extent is decreasing; lake and river ice freeze-up dates are occurring later and breakup dates earlier; glaciers are retreating rapidly; sea-ice extent is at record minimums and thinning; and permafrost temperatures are increasing and, in many cases, permafrost is thawing. In the context of greenhouse gas emissions, permafrost (i.e. soil or rock that has remained below 0 °C for a minimum of two consecutive years) thawing could contribute to the release of a significant amount of $CH_4$ and $CO_2$ stored in organic frozen soils (Christensen et al., 2004; Serreze et al., 2000).

Surface temperature is an essential measure for understanding biological, hydrological and climatological systems that operate through interaction and feedback mechanisms and which cannot otherwise be fully understood when considered separately. Surface temperature reflects the results of surface-atmosphere interactions and energy exchanges between the atmosphere and the ground (Williams and Smith, 1989). In regions underlain by permafrost, it is a critical variable for understanding the thermal regime of the ground. For that purpose, surface temperature is used in spatially-distributed models describing the thermal regime of permafrost (Sazonova and Romanovsky, 2003). To date, however, temperature fields used as input in such models have largely been derived through spatial interpolation of near-surface air temperature measurements from a limited number of geographically scattered meteorological stations (e.g. Hinzman et al., 1998; Shiklomanov and Nelson, 2002) or, more recently,





TCD
5, 1583–1625, 2011



have been provided by coarse resolution (e.g. 2.5° latitude × 2.5° longitude) atmospheric reanalysis data such as NCEP/NCAR (Shiklomanov et al., 2007). These data are either not spatially representative (field) or too coarse (reanalysis) for regional permafrost studies. Satellite remote sensing sensors operating in the thermal infrared part of the electromagnetic spectrum are of particular interest since they offer the potential to retrieve land surface skin temperatures (LST) on a daily basis over large areas at the 1 $km^2$ horizontal resolution.

Interest is currently being expressed by the permafrost science community to use satellite-derived LST either as a replacement or in conjunction with more spatially limited near-surface air temperature measurements from meteorological stations in permafrost models (Romanovsky, pers. comm., 2010). There has also been interest for some time already in using spaceborne LST measurements for climate monitoring at high latitudes. A few studies have utilized LST obtained from satellite sensors (NOAA AVHRR, GOES, and SSM/I) to observe temperature variability and trends in Boreal and Arctic regions (Comiso, 2003, Goïta et al., 1997; Han et al., 2004; Mialon et al., 2007, Traoré et al., 1997). LST products derived from the Moderate Resolution Imaging Spectroradiometer (MODIS) are increasingly being used to study various land components and processes at northern latitudes. Recent applications include vegetated areas (Coops et al., 2009), $CO_2$ exchange (Schubert et al., 2010), and permafrost at regional (Hachem et al., 2009) and local scales (Langer et al., 2010; Westermann et al., 2011).

MODIS 1-km LST products have been verified (compared) or validated against ground-based temperature measurements over homogeneous areas such as lakes (Wan et al., 2002a, b; Wan et al., 2004; Hook et al., 2007; Wan, 2008; Crosman and Horel, 2009), rice crops (Coll et al., 2005, 2009; Wan et al., 2004; Galve et al., 2007), silt-playa (Snyder et al., 1997), and densely vegetated areas (Wan, 2008). The 1 km products have also been validated with the alternative radiance-based (R-based) method over a lake and rice crops (Wan and Li., 2008; Coll et al., 2009) and dense forest (Coll et al., 2009). In addition, comparisons have been conducted between near-





TCD
5, 1583–1625, 2011



surface air temperature measurements at meteorological stations and MODIS 5-km LST products, and upscaled to 25 km, around the globe (Bosilovitch, 2006). Most validations/comparisons have been made at mid- and low-latitude sites. Recently, Langer et al. (2010) and Westermann et al. (2011) compared summertime MODIS LST data with those obtained with a thermal imaging system installed on a mast 10 m above the ground at two permafrost sites. They report differences of less than 2 K between the two sets of measurements under clear-sky conditions, with occasionally larger differences when clouds are not properly detected in the MODIS LST product.

The objective of this research was to compare the 1-km LST product (i.e. the clear-sky "skin" temperatures) retrieved from the MODIS sensor aboard the Terra and Aqua satellite platforms to near-surface soil and air temperatures measured year-round at meteorological stations. In the same way as in Bosilovich (2006), the purpose of this study is to verify the correspondence between meteorological station and MODIS data as to establish a more general relation than through validation using thermal radiometers or imaging systems which, unlike near-surface air temperature measurements, are limited temporally (summer only) and to very few sites (e.g. Langer et al, 2010; Westermann et al., 2011). The sites are located in high latitude regions characterized by heterogeneous tundra surface types in the continuous permafrost zone of northern Québec, Canada, and the North Slope of Alaska, USA.

## 2 Data and methods

### 2.1 Rationale for the selection of MODIS on the terra and aqua platforms

#### 2.1.1 Land surface temperature retrieval from various satellite sensors

Surface temperature can be retrieved from satellite sensors based on the use of the split-window method. This method is based on algorithms that utilize the differential absorption of two adjacent spectral windows (channels around 11 and 12 µm). The





TCD
5, 1583–1625, 2011



reason for choosing these windows is that the atmospheric attenuation is greater in the 12 µm channel than the 11 µm channel, and that the difference between radiances in these two channels augment with an increase in the atmospheric attenuation (Becker and Li, 1990a). Since the radiance of the surface being sensed does not change, the increased difference between the two radiances is related to atmospheric attenuation (Becker and Li, 1990a; Kerr et al., 1992; Ouaidrari et al., 2002). Hence, it should be possible to calculate surface temperature from satellite thermal infrared measurements acquired at 11 and 12 µm using a split-window equation.

However, two unknowns need to be determined using the split-window approach: the emissivity of the surfaces under consideration in both channels and the atmospheric transmission. The atmospheric transmission can be determined either using atmospheric transmission models (e.g. MODTRAN or LOWTRAN) for various atmospheric moisture conditions (Becker and Li, 1990a, 1995; Wan and Dozier, 1996; Goïta and Royer, 1997; Ouaidrari et al., 2002), derived from direct measurements of water content based on radiosondes (Goïta and Royer, 1997), or from sensors sensitive to atmospheric water content (e.g. HIRS/2 for the Advanced Very High Resolution Radiometer, AVHRR). The atmospheric transmission can also be derived directly from the same sensor such as the Moderate Resolution Imaging Spectro-radiometer (MODIS) which acquires data in multiple channels; some of which are used to detect particles in suspension in the atmosphere (Wan and Dozier, 1996; Justice et al., 1998). The atmospheric concentrations are retrieved from the MODIS atmospheric product (MOD07_L2), (Wan, 2007). As for the emissivity of land surfaces, it usually varies between 0.9 and 1. Similarly to the correction of atmospheric attenuation, several methods have been developed to derive surface emissivity. As an example, its estimation from AVHRR can been done using the Temperature Independent Spectral Index (TISI) (Becker and Li, 1990b; Li and Becker, 1993). The TISI approach uses the bidirectional reflectance in channel 3 (at 3.7 µm) of AVHRR measured day and night, and assumes that the bidirectional reflectance distribution function (BRDF) and atmospheric profiles are known (Wan and Li, 1997). The MODIS LST products make use of other available





TCD
5, 1583–1625, 2011



MODIS-derived products. For example, emissivities are estimated by the classification based emissivity method (Snyder et al., 1998) according to land cover types in the pixel determined by the input data in the MODIS quarterly land cover (MOD12Q1) and daily snow cover (MOD10_L2) products (Wan, 2007). With the MODIS sensors aboard NASA's Aqua and Terra satellites, maximum surface temperature errors have been reported to range between 2 and 3 K, with a standard deviation of 0.009 due to emissivity errors in bands 31 and 32 (infrared region of 10 to 12.5 µm) (Wan and Li, 1997).

### 2.1.2 High temporal and spectral resolution, and moderate spatial resolution

The NOAA satellite series as well as the Terra and Aqua satellites possess a twice-daily repeat overpass and a 1 km spatial resolution in the thermal infrared. The twice-daily temporal resolution is of particular interest as it allows one to monitor the evolution of surface temperatures throughout the year. Regions of the Arctic are rather thermally homogenous on the scale of tens of kilometers, which makes the spatial resolution of 1 $km^2$ satisfactory and precise enough to cover vast territories. At the pixel scale (within a 1 $km^2$ grid-cell), however, variations in topography, surface materials, vegetation and snow cover can influence the temperatures measured from spaceborne thermal sensors.

The first NOAA satellites were launched in 1979, providing a long time series for studying Arctic climate change over a period of more than 25 years (Comiso, 2003). However, a temporal drift is known to occur during the lifetime of NOAA satellites which can result in a local overpass time variation of up to 4 h, especially in the afternoon (Traoré et al., 1997). This orbital drift results in a significant cooling of the LST measurements (Gleason et al., 2002; Jin and Treadon, 2003). The Terra and Aqua satellites, which have been active since 2000 and 2002, respectively, do not suffer from such drift. Although both the AVHRR and MODIS sensors possess the same 1-$km^2$ spatial resolution in the thermal infrared, the LST from the Terra and Aqua satellites were chosen for this study rather than those provided by NOAA AVHRR. This choice thus directs the research towards the evaluation of a relatively new product (MODIS LST)





TCD
5, 1583–1625, 2011



for land-surface temperature mapping in the Arctic rather than a time series analysis of trends and variability in surface temperatures with climate.

MODIS possesses another advantage over AVHRR in that it acquires data in 36 channels, which provides emissivity simultaneously with thermal infrared reflectivity (used to calculate surface temperatures) and short infrared (used to calculate atmospheric water contents), thus reducing errors in LST and cloud cover. In addition, the spatial resolution of 1 km allows the Earth's surface to be covered in 1 day with a frequency of acquisition of as much as 4 times per day if Terra and Aqua data are combined. Thus, the more frequent coverage can improve the calculation of a mean daily LST, which is of particular interest to permafrost mapping and modeling efforts.

### 2.2 Location of study sites and data description

All ground-based meteorological stations for this study were located in tundra areas underlain by continuous permafrost, north of treeline, in northern Québec (Canada) and northern Alaska (USA). The characteristics of each site for which near-surface soil and air temperature measurements were compared to MODIS LSTs are given in Table 1. The period of comparison was limited to the period 2000–2008 since MODIS LSTs from Terra are available starting in 2000. At some stations the air/soil temperatures from meteorological stations were only available until the end of 2003, for other stations until 2007 or 2008.

#### 2.2.1 Nunavik stations (northern Québec, Canada)

Five meteorological stations within three Inuit villages recorded hourly soil ($T_{soil}$) (3–5 cm below ground) and air ($T_{air}$) (1–2 m above ground) temperatures corresponding to Terra and Aqua overpass times during the period 2000–2008 (Fig. 1). Three stations are located near the village of Salluit: Sila, Tiki (for Tikiraatsiaq), and the Salluit Airport (SalA in Table 1). The fourth station is situated in Kangiqsualujjuaq on the southeast coast of Ungava Bay and the fifth station, operated by Environment Canada, is located





TCD
5, 1583–1625, 2011



in Kuujjuaq.

Northern Québec sits on the Canadian Shield. The soils overlying the glacially eroded bedrock are generally thin. Landforms of glacial origin are characterized by till-overlain plateaus, coastlines with sands of marine origin, and coastal valley bottoms with glaciomarine clays. At Salluit, plateau vegetation is composed of mosses and lichens with herbaceous plants dominating the valleys with fine soils. Occasional scattered shrubs dot slopes that are sheltered from the wind and covered by snow in the winter. Aerial views show a predominance of mosses and lichens interspersed with islands of bare soil or low shrubs. The meteorological stations at Salluit (Sila, Tiki and SalA) are situated in environments exposed to wind, which reduces the accumulation of winter snow to a thin (5–10 cm) cover. The Sila tower is located 1.75 km from the coast at an altitude of 45 m. It is installed on a small till hill surrounded by clay soils. Tiki is located 110 m from the coast on a rocky promontory advancing into a fjord at an altitude of 35 m. The area surrounding the tower consists primarily of lichen-covered bedrock and thin gravelly soils. The Salluit airport meteorological station (SalA) is found on the top of a plateau surrounding the village at an altitude of 225 m. The area around the tower consists of bedrock covered with patches of till and close to the runway. Kangiqsualujjuaq is found at the limit between the continuous and discontinuous permafrost zones. Trees with upright growth forms become more prevalent on hill slopes in this area. Palsas are found at the southern edge of the village. The area immediately surrounding the Kangiqsualujjuaq meteorological station is composed of bedrock and till that support lichens and prostrate scrub, i.e. shrub birch of 20–30 cm (Bouchard, 1990; Gahé, 1987) colonizing a thin till overlying gneissic rock (Table 1).

### 2.2.2 Stations within the Kuparuk River watershed (North Slope of Alaska, USA)

Sites in the Kuparuk River watershed extend along a 250 km north-south transect (Fig. 1). The transect is characterized from north to south by moss and lichen vegetation at Betty Pingo, herbaceous vegetation at Franklin Bluff, and shrub vegetation at Sagwon. An in-depth description of the sites can be found on the Water and





TCD
5, 1583–1625, 2011



Environmental Research Center (WERC) website[1]. In addition, Jia and Epstein (2004) provide a general description of Alaska's North Slope region in which the Kuparuk River basin is located.

### 2.3 Location of MODIS pixels corresponding to the meteorological stations

The LSTs from the MODIS sensor are derived using a day-night split-window technique that considers variations in emissivity as a function of time and measured in the same bands as those of the thermal infrared, i.e. channel 31 (10.78–11.28 µm) and channel 32 (11.77–12.27 µm) (Wan and Dozier, 1989, 1996; Wan et al., 2002; Wan, 2008). Surface temperatures calculated using this algorithm and with an already applied cloud cover mask are available from NASA's Warehouse Inventory Search Tool website[2]. The V5 level 3 MODIS LST (MOD11A1 and MYD11A1) products were used in this study.

MODIS pixels centered on or located close to the meteorological stations were selected for temperature comparisons. The presence of water bodies of different sizes in the proximity of certain stations can result in a mixed MODIS pixel over a given station. For example, a 1 $km^2$ pixel containing a higher water fraction than land can introduce some difficulties when comparing a satellite pixel with a measurement from the meteorological station which is located on land.

For meteorological stations located along the shore of water bodies that have an area greater than 1 $km^2$ (West Dock, Franklin Bluff, Western Kuparuk, Imnavait Basin, Tiki, and Kangiqsuallujjuaq), two MODIS pixels, one which contains the geographic coordinates of the station ("1" is added after the station name) and another one within

[1]WERC website: http://www.uaf.edu/water/

[2] Site homepage: https://wist.echo.nasa.gov/api/; names of products used: MODIS/TERRA LAND SURFACE TEMPERATURE / EMISSIVITY DAILY L3 GLOBAL 1KM SIN GRID V005 and MODIS/AQUA LAND SURFACE TEMPERATURE / EMISSIVITY DAILY L3 GLOBAL 1KM SIN GRID V005





TCD
5, 1583–1625, 2011



2 km of the station ("2" is added after the station name), were chosen (Table 2).

For the northern Québec sites, the water fraction within each MODIS pixel was determined using the Canada-wide 1-km water fraction data product from National Topographic Data Base Maps (NTDB) (Fernandes et al., 2002). This raster product gives a percentage for the fraction of water contained in each 1 $km^2$ pixel. The surface category types were established using NTDB maps at the scale of 1/50 000 and 1/250 000. "The majority of NTDB source maps was surveyed within the growing season (post snow-melt) and should therefore be relatively unbiased during the growing season in the absence of drought or severe precipitation events"[3]. Only the open water category was retained for the determination of water fraction within each 1-km grid cell (i.e. humid zones, wetlands, and small ponds are excluded). Thus, one must keep in mind that the MODIS LST for some sites may be influenced by variations in surface wetness/moisture (seasonally and annually) even if the water fraction given in the NTDB raster product corresponds to 0 %. MODIS pixels corresponding to the coordinates of the stations Tiki, Sila and Salluit airport contained 100 %, 9.7 %, and 0 % of water, respectively. The pixel containing the Sila tower is called Sila1, the one that includes the Tiki station is referred to as Tiki1 and the one with Salluit airport station is called SalA1 (Table 2). The pixel named Tiki2 is situated one pixel south of Tiki1 and contains less water (17.5 %). At Kangiqsuallujjuaq, the pixel centered on the station has a water fraction value of 10.4 % (Kangiq1). Hence, an adjacent pixel with 8.9 % water coverage was chosen (Kangiq2). At Kuujjuaq, the pixel corresponding to the village coordinates had 0 % of water on the Water fraction map (site Kuujjuaq1). Unfortunately, it had no LST values recorded from 2000 to 2008. Hence, two other pixels were chosen with also 0 % of water. One is situated at the pixel on the left and down of the original position (Kuujjuaq2) whereas the second one is on the right (Kuujjuaq3).

A map of land surface types of the North Slope of Alaska was used as an aid for selecting pixels corresponding to stations located in the Kuparuk River watershed. The map used is the Land-Cover Map of the North Slope of Alaska[3] which represents soil

[3]This map is accessible via the NSIDC website : http://nsidc.org/data/arcss020.html





TCD
5, 1583–1625, 2011



and vegetation types. Nine categories were found in this map, one of them corresponded to "water". The map was derived from the classification of a mosaic of Landsat MSS images resampled at 100 × 100 m spatial resolution. The Landsat images were acquired during the snow-free period of the growth season (i.e. July, August, or September, depending on the year). Water bodies could readily be identified and water fraction determined for each MODIS pixel (i.e. 100 Landsat pixels within one MODIS pixel). The water fraction, expressed in percent, was determined for each site: West Dock (WD1: 57.5 % – WD2: one pixel south with 28.1 % water), Betty Pingo Upland (BPU1: 1.5 %) and Wetland (BPW1: 17.9 %), Upper Kuparuk (UK1: 2.2 %), West Kuparuk (WK1: no standing water; but as the vegetation is highly wet, another pixel with less percent of wet vegetation was taken – WK2: one pixel north with 7.2 % water). For the same reason (Table 2), two pixels were selected for Franklin Bluff (FB1 and FB2) even though both of them had 0 % water fraction reported. The digit "1" was added at the end of the names of the sites to indicate that the pixel extracted corresponded to a pixel that included the meteorological station location, while digit "2" (or "3") was added for an immediately adjacent pixel containing less water.

### 2.4 Comparison between MODIS LST and near-surface soil/air temperature measurements at meteorological stations

$T_{soil}$ and $T_{air}$ measured at the northern Québec and Alaska stations were compared to the MODIS-derived LST. When hourly measurements from stations were available concurrent with the time of MODIS data acquisitions, it was possible to compare the ground-based $T_{air}$ and $T_{soil}$ measurements with those acquired at the time of Terra and Aqua overpasses above the stations. In fact, MODIS data are not continuous; it was found that many consecutive days were without retrieved LST values. This is due to the many days with cloudy conditions over the study areas (Table 3). For the period when only Terra was in orbit (2000–2001), cloudless days accounted for only 5 to 19 % (average of 12 %) and 23 to 32 % (average of 28 %) of the MODIS observations over northern Québec and Alaska, respectively, depending on the location of the





TCD
5, 1583–1625, 2011



meteorological stations. When MODIS observations from both Terra and Aqua became available, starting in 2002, the percentage of cloudless days increased to 20 % on average over the Québec stations and about 46 % over the stations located in Alaska.

Two statistical parameters were computed to compare MODIS LSTs with temperature measurements from meteorological stations: the Pearson correlation coefficient (R) and the mean difference (MD). The correlation coefficient was used as a measure of the temporal coherence/match (co-variation in time) between the satellite and station temperature measurements. The mean difference was utilized as a measure of the difference between the two sets of data. It is equal to zero when the mean LST is equal to the mean soil/air temperature. If the mean difference is positive, the mean LST is larger (warmer) than the mean soil/air temperature. Inversely, if the mean difference is negative, then the mean LST is colder than the mean station temperature measurement. It is important to note prior to analyzing the results that the MODIS LSTs are being verified/compared, not validated, against the temperature measurements from the meteorological stations. Strictly defined, validation would require the deployment of thermal infrared (TIR) radiometers within the 1-km$^2$ resolution of the MODIS pixels that encompass the field sites.

## 3 Results

Each MODIS LST data series (Aqua-day, Aqua-night, Terra-day, and Terra-night) was first compared with soil and air temperatures taken at each station within the hour of the satellite overpass. Firstly, correlation and mean difference values between MODIS LSTs and the hourly temperatures at stations, when available, were calculated. This allowed a verification of the mean morning (LST-day) and the mean evening (LST-night) LSTs for Aqua and Terra. Secondly, mean daily temperatures from the stations and from Terra and Aqua LSTs (LST-day/night) individually, and then combined (mean Terra and Aqua), were calculated (Figs. 2–4). Finally, comparisons were also made seasonally (winter and summer) and on an annual basis (Fig. 5).





TCD
5, 1583–1625, 2011



As indicated in Table 4, the two satellites pass more frequently over Alaska between 10:00 and 12:00 and over northern Québec between 11:00 and 13:00 at their ascending overpasses. Whereas, during their descending overpasses, Aqua passes over Alaska around 00:00 and 02:00 and over northern Québec between 02:00 and 03:00; and Terra passes over Alaska between 19:00 and 21:00 and over northern Québec between 21:00 and 22:00. In reality, overpass times are not on the hour. However, to simplify the comparison with station measurements a fixed hour, defined as the interval that includes the half-hour before and after an overpass, was given. As a result, satellite data acquired between 10:30 and 11:30 are used for comparison with hourly station measurements from 11:00.

### 3.1 Near-surface soil temperature

MODIS LST data were first compared with near-surface soil temperature measurements. The near-surface soil temperature is measured just under ground at around 3 cm deep (to be protected from bad weather and direct radiations). Six of the ground-based stations were equipped with data loggers measuring hourly soil temperatures (Sila, Tiki, Betty Pingo Upland, Betty Pingo Wetland, Franklin Bluff and Sagwon) while at two other stations (Ivotuk shrub and Ivotuk moss) soil temperatures were recorded every 3 h. At West Kuparuk, Upper Kuparuk and Imnavait Basin only average daily temperatures were recorded. There were no near-surface soil temperature measurements available at West Dock, Salluit Airport (SalA), and Kuujjuaq (Table 1).

#### 3.1.1 Comparison of daytime and nighttime temperatures

MODIS retrieved LSTs over Salluit and the Kuparuk River Basin are well correlated with $T_{soil}$ within the hour of overpass for either the ascending (daytime overpass) or the descending mode (nighttime overpass) (Table 4). LSTs are in good agreement at daytime for Terra ($0.76 < R < 0.96$; $-8.72<MD<6.03$ with mean of $-2.71$) and for Aqua ($0.81< R <0.97$; $-8.10<MD<5.05$ with mean of $-3.27$). At nighttime, the correlation is





TCD
5, 1583–1625, 2011



as good as at daytime but the differences are colder for Terra ($0.82 < R < 0.96$; $-10.47 < \mathrm{MD} < -3.98$ with mean of $-7.36$) and for Aqua ($0.72 < R < 0.99$; $-13.02 < \mathrm{MD} < -4.06$ with mean of $-8.72$) with soil temperatures. The mean difference is larger during nighttime; the LSTs being 3–4 °C colder than daytime for some Alaskan stations and for Sila and Tiki. 13:00 and 14:00 are the hours at which the mean differences between LST and $T_{soil}$ are the smallest and the correlations are the highest, independently of the station in Alaska, while it is at 12:00 for the Québec stations.

#### 3.1.2 Comparison with mean temperatures calculated from Terra and Aqua combined

The temperature measurements taken by Terra and Aqua are close to each other during daytime and nighttime for all stations over the entire study period, despite the different overpass times of the two satellites. The two overpass times for each satellite (daytime and nighttime) allow for the possibility of four temperature measurements over a 24-h period, providing for the calculation of a mean daily temperature that closely approaches the mean daily temperature measured at the ground stations. In order to calculate the mean daily temperature from the data of the two sensors, we first calculated separately the mean LST-daytime of Terra ($0.84< R < 0.95$; $-6.97 < \mathrm{MD} < 1.00$ with mean of $-2.71$) and Aqua ($0.85 < R < 0.95$; $-8.19 < \mathrm{MD} < 0.62$ with mean of $-3.27$) and the mean LST-nighttime for Terra ($0.85 < R < 0.94$; $-9.15 < \mathrm{MD} < -5.89$ with mean of $-7.36$) and Aqua ($0.85 < R < 0.94$; $-10.75 < \mathrm{MD} < -7.42$ with mean of $-8.72$). When only one sensor had recovered a temperature for a given time period, that temperature alone was used. In other cases, the mean daily temperature was determined using the daytime LST retrieved by Aqua and the nighttime LST obtained by Terra, and vice-versa. The intent was to have the maximum number of LST measurements per day.

At Salluit, for the Terra and Aqua Day-Night the $R$ value (0.96) is higher than the average in Alaska ($0.86< R <0.95$). At Salluit, the mean difference indicates that LSTs are 3 °C lower than $T_{soil}$ ($-2.83$ at Tiki2 and $-3.38$ at Sila1). At the Alaskan stations,





TCD
5, 1583–1625, 2011



for the Terra and Aqua Day-Night average, the mean difference indicates that LSTs are 5–9 °C colder than $T_{soil}$ ($-8.56 < MD < -4.70$). Here, it can be established that the relation between $T_{soil}$ and LST with mean LST-Day/Night increases only weakly the relation with $R$ values ranging from 0.86 to 0.96.

In addition, the average LST-Day/Night and Aqua-Terra (AqTeDN) shows a better relation than the nighttime data but a worse relation than the daytime data. Even if the correlation looks very good at some hours of the day, when plotting the LSTs and $T_{soil}$against dates (Fig. 3), it appears that differences are larger in summer than in winter. Regionally, the relation between the $T_{soil}$ and LST for the Alaskan stations is not as strong as the one for the Québec stations.

### 3.2 Near-surface air temperature

MODIS LST data are also compared with near-surface air temperature measurements ($T_{air}$). These data are measured at 1–2 m above the ground under shelter. Most of the stations (except Betty Pingo Wet and Imnavait Ridge) have such instrumentations (Table 1).

#### 3.2.1 Comparison of daytime temperatures

The best relation between the two types of temperature measurements is obtained in the middle of the day in both Alaska and Québec. In Alaska, Terra overpasses between 10:00 and 15:00 giving $R$ values ranging from 0.93 to 0.98 and MD between −3.07 and 0.29 (with mean of −0.70 over the 2000–2008 period), while Aqua overpasses between 9:00 and 14:00 resulting in $R$ values between 0.93 and 0.99, and MD from −3.65 to 0.16 (with mean of −1.21). Over Québec, Terra overpasses between 10:00 and 13:00 leading to $R$ values ranging from 0.93 to 0.97 and MD ranging from −1.18 and 1.65 (with mean of 0.39), while Aqua overpasses between 11:00 and 13:00 giving $R$ values ranging from 0.91 to 0.98 and MD from −0.34 and 2.60 (with mean of 1.12) depending on the station (Table 5 and Fig. 4).





TCD
5, 1583–1625, 2011



In Figs. 6–7, the daytime LST (in red), the nighttime LST (in blue) and the mean LST-day/LST-night (in green) are superimposed on the 24-h mean air temperature curves of two different stations (Imnavait Basin and Kuujjuaq). In these graphs, the LST-Day is situated slightly above $T_{air}$ and is most pronounced during the summer period. In the positive areas of the graphs, where summer temperatures are found, clusters of LST-Day values are always at temperatures higher than those of LST-Night. In the negative areas, which correspond to winter, the clusters of LST-Day and LST-Night show similar temperatures. Figures 6 and 7 clearly show the tendency of the MODIS-derived temperatures to be warmer than near-surface air temperatures during the summer months.

### 3.2.2 Comparison of nighttime temperatures

At nighttime, Aqua passes between 00:00 and 05:00 and Terra between 18:00 and 23:00 over the Kuparuk River Basin, while over northern Québec (Nunavik), Aqua passes between 00:00 and 04:00 and Terra between 20:00 and 23:00. As revealed in the graphs (Figs. 6–7), the correspondence between the MODIS LST and near-surface air temperatures at the stations is overall weaker during nighttime (18:00 to 05:00) than during daytime (09:00 to 15:00). $R$ values at nighttime fluctuate for Terra between 0.92 and 0.97 in Alaska, and between 0.87 and 0.96 in Québec, while for Aqua the $R$ values fluctuate between 0.90 and 0.98 in Alaska and between 0.90 and 0.97 in northern Québec depending on the station. The mean differences during nighttime are much more negative than during daytime in both study areas (Alaska: $-6.39 < \text{MD Terra} < -1.30$ with mean of $-2.87\,^{\circ}\text{C}$, and $-7.66 < \text{MD Aqua} < -2.65$ (mean of $-4.57$), and in Québec: $-5.95 < \text{MD Terra} < -3.83$ (mean of $-5.43$), and $-7.72 < \text{MD Aqua} < -4.21$ (mean of $-6.11$), pointing out an important variance between LST-Night and $T_{air}$ night. LSTs are smaller (colder) than the $T_{air}$ at night. In Figs. 6–7, the LST-Night is more often below the $T_{air}$ either in summer or winter. These figures show that in winter the LST-night appears to follow the slope of the mean daily temperature curve fairly accurately. In contrast, in summer, although the LST-night is never above the mean daily temperature curve, a large number of the MODIS temperature measure-





TCD
5, 1583–1625, 2011



ments are much colder than near-surface air temperatures. The nighttime differences for all stations combined over the entire study period vary between −7.72 and −1.3 °C.

### 3.2.3 Comparison with mean temperatures calculated from Terra and Aqua separately

As shown earlier, MODIS LST-Day values tend to be warmer than the mean daily temperatures while the LST-Night values tend to be colder. It is therefore worth examining how a mean value calculated from both LST-Day and LST-Night temperatures compares to the mean daily air temperature ($T_{air}$) obtained from station measurements (Table 5). Using the mean of the two LSTs (average of daytime and nighttime values) the $R$ values of Terra vary between 0.95 and 0.98 in Alaska, and between 0.92 and 0.98 in Québec, with a MD between −4.89 and 0.02 °C (mean of −1.37) in Alaska and between −2.80 and −1.05 (mean of −1.71 °C) in Québec. For Aqua, the $R$ values vary between 0.96 and 0.99 in Alaska and between 0.94 and 0.98 in Québec, with a MD between −5.86 to −1.44 (mean of −2.69) in Alaska, and between −2.36 and −0.66 (mean of −1.28 °C) in Québec. This shows a general tendency of mean LST to be below the average daily $T_{air}$.

### 3.2.4 Comparison with mean temperatures calculated from Terra and Aqua combined

The calculation of the mean greatly reduced the number of anomalous LST values that we believe are related to undetected clouds. If one of the two sensors "observed" a cloud during the day, and therefore did not record a land surface temperature, while the other retrieved a very cold surface temperature, it would still be moderated by the LST-night. However, it is possible that the two satellites did not identify the presence of clouds, in which case the mean LST would still be calculated. Calculating a daily average by combining both Terra and Aqua data results in a better match with $T_{air}$, with $R$ ranging from 0.93 to 0.99 and MD from −5.13 to −0.51 (mean of −1.86 when all





TCD
5, 1583–1625, 2011



stations from Alaska and Northern Québec are pooled together).

## 4 Discussion

### 4.1 Temperature differences in winter and in summer

#### 4.1.1 Comparison of MODIS LST with near-surface soil temperatures: large differences during the transition seasons

Differences between the low correlations of LST vs. $T_{soil}$ at Kuparuk compared to those in Salluit can be explained by the fact that the temperatures derived from MODIS are clear-sky skin temperatures, i.e., the temperature at the air-soil (snow-free) or air-snow interface. They, as expected, do not correspond exactly to the temperatures measured at the stations where the temperatures were taken at 2–3 cm depths in order to provide protection from the elements and wildlife. However, it is in these first few centimeters that temperatures are the most variable in time and space (Figs. 3–4).

$T_{soil}$ represents the heat transfer equilibrium related to molecules agitation between two systems, while the surface temperature obtained from satellite sensors is determined from surface brightness temperature and surface emissivity after atmospheric corrections have been applied. The soil can be covered by vegetation (low or high), an organic layer and snow which act as buffer layers which have an impact on thermal exchanges with the atmosphere above by decreasing or increasing the ground temperatures, depending on the season. During the freezing period, the energy transfer occurs in the form of latent heat. The soil temperature decreases only through the release of energy which takes some time (i.e. the time necessary to convert all water into ice), and inversely in spring, during the melting period. In winter, the "zero curtain" is strongly dependent on the arrival of snow. If it is early, before the first freeze, the snow insulates the ground from cold air temperatures. Then, to decrease the soil temperature, the air temperature must be sufficiently cold to be conducted through the





TCD
5, 1583–1625, 2011



snow layer before starting to freeze the ground. On the other hand, if snow arrival is late, the soil has already started to freeze before the snow starts to play its insulation effect. As seen in the regression plots of Fig. 3, the "zero curtain" associated with the effect of snow occurred when many field temperatures have values at 0 °C, while MODIS continues to measure temperatures between −20 and +10 °C. This effect is relatively long, as it persists for approximately one month at the Betty Pingo, Franklin Bluff and Western Kuparuk sites. The temperatures at Sila were also taken at a depth of 3 cm, and the "zero curtain" effect is also visible (Fig. 3), but to both a lesser extent and shorter period of time (less than one week). This is due, at Salluit, to a more rocky landscape with less water content in the soils and with the temperature probes being located in windy corridors where snow is blown; this factor results in less time required for water state changes at the beginning and ending of the thawing season. Furthermore, if the correlation at Sila is especially high (0.96) it is also because the satellites only acquired a few scattered measurements for the time period when this effect occurred (mid-October to mid-May). Thus, there were only a few measurements corresponding to the "zero curtain" period.

During spring, the insulation effect of snow is less efficient because of the denser snow cover and the likely presence of ice lenses/crusts due to diurnal freeze and thaw cycles. The transition period in spring takes less time, just 10 days for the Kuparuk River Basin stations and one week at Salluit.

#### 4.1.2 Comparison of MODIS LST with near-surface air temperatures

There is a tendency for nighttime LST to be colder than $T_{air}$ throughout the year by −1.96 to −6.94 °C (depending on stations), with a mean night difference of −1.86 °C (Fig. **??**) which occurs as result of heat transfer (radiative cooling) from the ground surface to the air above at night. Also, the role of annual changes in day length is important in the Arctic. "LST-Day" during winter corresponds to days without sunlight. Actually, overpass times at 09:00, 10:00, and 15:00 are "nighttime" acquisitions for many of these stations. This, plus the low sun angle during daylight, explains why





TCD
5, 1583–1625, 2011



there is less difference between day and night temperatures in the winter. In the summer, even though the sun is above the horizon for much of the day, the sun zenith angle varies enough to make "day" temperatures warmer than "night" temperatures (which, for a part of the night hours, are sunlight hours). Therefore, the separation of the year into two parts (summer and winter periods) does not take into account the difference in day lengths. We considered the summer period to start on 1 June and end on 30 September, to include the growing season as determined by Zhou et al. (2001). This period includes the summer solstice (almost 20 h of daylight) and ends close to the autumn equinox (21 September), which means that during this period the maximum day length is reached for meteorological stations above 60° N. In turn, during this period, nights are very short. On the other hand, during the cold season (1 October–30 May, there are few hours of daylight, except in spring at the vernal equinox. For instance, the city of Fairbanks, Alaska (about 65° N) has 21 h of daylight 10 May–2 August and only 4 h between November 18 and 24 January.

There appear to be differences between the LST taken in summer and winter according to the shape of the distributions in the plots of Figs. 6–7. The transitional snow melt and frost periods, which last between ten days to a month at these high latitudes, were included in the winter season. Thus, in the middle of winter, the frozen snow-covered landscape is relatively homogeneous and, as a result, the complicating effects of soil and surface wetness are absent; the LST values represent those at the air-snow interface. However, it is different at the beginning and end of the defined winter season (1 October–30 May ), in particular for the period corresponding to the beginning of snowmelt and active layer thaw when extensive areas of stagnant water form due to the impermeability of the underlying frozen soils. The presence of the stagnant water modifies the heat exchanges between the soil surface and the atmosphere at the soil interface, which the 2-m height air temperatures do not measure. Including the period of snowmelt it is one of the reasons why the temperature differences in summer are fluctuating around 0 °C ($-1.34 < MD < .66$ with a mean of 0.52 °C) (Fig. 5). During snowmelt the LST better represents the near-surface (melting snow) temperature than





TCD
5, 1583–1625, 2011



the $T_{air}$. As it has been seen previously, the temperature of undetected clouds is lower than that of air temperature and can lead to larger differences, which provides some of the explanation for the differences in winter ($-7.18 < MD < -1.11$ °C with a mean of $-2.98$ °C). Also, in summer, $R$ values below 0.75 for 4 stations (6 pixels) – West Dock (WD1 and WD2), Tiki (Tiki2), Kangiqsuallujjuaq (Kangiq1 and Kangiq2) and Kuujjuaq (Kuujjuaq2) show a weaker relation between LST and $T_{air}$ (Fig. 5). As an example, in Fig. 8, the graphs for the WD1 site show the temperature differences in summer and winter. For the other stations, $R$ values are all above 0.75 (up to 0.94). The presence of subgrid-scale water (see Table 2) within the MODIS pixels explains the more moderate relations between LSTs and 2-m height air temperature measurements at some of the sites. Globally, the temperature differences are larger in winter than in summer (Fig. 5). Summer differences are more frequently above 0 °C which means that LSTs are higher than $T_{air}$ during this season ($-1.34 < MD < 1.66$ with a mean of 0.52 °C). In winter, differences show an opposite tendency. LSTs are colder than $T_{air}$ ($-7.18 < MD < -1.11$ °C with a mean of $-2.98$ °C). In absolute term, the differences in summer are smaller than during winter (Fig. 5) for all stations.

Fluctuations in soil temperatures are dependent on fluctuations in surface temperatures, which are in turn influenced by atmospheric temperatures. Thus, at different time scales, it is possible to define different fluctuation periods. A period of one year corresponds to the annual solar radiation cycle while a period of one day corresponds to the diurnal solar radiation cycle (Williams and Smith, 1989). The difference between LST and $T_{air}$ can be large over a diurnal cycle, while it diminishes over a monthly cycle. Seasonally, there is a slight tendency to yield a warmer summer temperature (+0.52 °C) and a colder winter temperature ($-2.98$ °C). The mean annual difference for all stations combined is $-1.84$ °C, with a propensity for the LST to be below $T_{air}$. Therefore, the LST are slightly warmer in summer and, to a greater magnitude, colder in winter.

It is clear from Fig. 5 that calculation of the mean annual LST removes the larger bias of the winter months by that of the summer months and that, as a result, LSTs become closer to $T_{air}$ when averaged over the year but still, the differences observed





TCD
5, 1583–1625, 2011



show clearly that they are two different variables (clear-sky satellite "skin" surface-air interface temperature vs 2–3 m height air temperature). The differences are largely due to the nature and state of the surfaces being sensed within the MODIS pixels (e.g. vegetation, bare rock, surface water and wetness). Overall, regardless of surface type, LST and $T_{air}$ show a high degree of temporal coherence and on broad spatial and temporal (over a year) scales they follow the same trajectory. Since mean annual air temperatures are very important for calculating the thermal regime of permafrost, the annual means of LST, similar to $T_{air}$, are seen as useful for permafrost studies.

## 5 Conclusions

The MODIS LST, as indicated by comparing with temperatures measured at meteorological stations, provides an excellent data source for regional monitoring of skin temperatures in Arctic regions at the resolution of 1 km$^2$. Correlations were found to be generally weaker and mean differences higher in winter than in summer for most stations. The weaker relations obtained between $T_{soil}$ and LST in winter as opposed to summer (or $T_{air}$ and LST) are due to zero curtain effect during transition periods (seasons) and to snow cover effects.

The MODIS temperature data were shown to be close to hourly near-surface air temperature measurements and even more to daily average temperatures (mean of LST-Day and LST-Night). The relation between the two sets of measurements is stronger and mean differences are smaller when data are averaged on a seasonal and even better on an annual time scale. Given this, and recognizing that the presence of clouds does not permit a continuous temporal coverage throughout a full annual cycle, the MODIS-derived LSTs are nonetheless a promising means for monitoring and modeling the surface thermal regime of regions underlain by permafrost. Although the amount of clouds can be significant in the Arctic such that it is impractical to retrieve LSTs with thermal infrared satellite sensors for several days to several weeks of the year, procedures have recently been developed (e.g. sinusoidal regression model) to replace





TCD
5, 1583–1625, 2011



missing data due to the presence of clouds in MODIS time series (Hachem, 2009). Alternatively, it may be possible to combine MODIS LSTs with temperature values obtained with coarser resolution passive microwave satellite data (e.g. Kohn and Royer, 2010; Royer and Poirier, 2010).

Actually, in permafrost studies, it is possible to use the mean annual air or surface (it is even better) temperature as input into mathematical models which reproduce the thermal regime into the ground. MODIS LSTs can also be used to calculate the sum of positive degree-days (thawing index) and the sum of negative degree-days (freezing index) (Hachem et al., 2008; Hachem et al., 2009), and therefore enable to estimate the seasonal evolution of the active layer thickness (i.e. the soil layer above permafrost which freezes and thaws seasonally). The LST can also be used to evaluate the surface temperature of large lakes to estimate their thermal regime and to verify against lake models used in numerical weather prediction and regional climate models (e.g. Kheyrollah Pour et al., 2011). Concerning vegetation, it has been shown that the threshold of growing season for black spruce is 800 degree-days above mean annual air temperature of 5 °C (Meunier et al., 2007). Using the LST, it is possible to evaluate above certain regions the growing season of black spruce. Other thresholds for other plant species could also make use of LST.

*Acknowledgements.* This research was supported by grants from the Natural Sciences and Engineering Research Council of Canada (NSERC), ArcticNet, and Ouranos. All MODIS Land Surface Temperature data were obtained through the WIST website operated by NASA. Field data from the Alaskan sites were obtained via the website maintained by the Water and Environment Research Center (http://www.uaf.edu/water/projects/NorthSlope/references.html), University of Alaska Fairbanks. Field data from the Québec sites were obtained through the SILA-SAON network of meteorological stations and thermistor cables operated by the Centre d'études nordiques, Université Laval (Québec), and data from Kuujjuaq were downloaded from Environment Canada's website http://www.climat.meteo.gc.ca/climateData/canada_e.html?\&. Special thanks are extended to K. Tessier, Université Laval, for her help with the reproduction of Fig. 1 and Normand Bussières, Environment Canada, for his comments on an earlier draft of this manuscript.





TCD
5, 1583–1625, 2011



## References


Becker, F. and Li, Z.-L.: Towards a local split window method over land surfaces, Int. J. Remote. Sens., 11, 369–393, doi:10.1080/01431169008955028, 1990a.

Becker, F. and Li, Z.-L.: Temperature independent spectral indices in thermal infrared bands, Remote. Sens. Environ., 32, 17–33, 1990b.

Becker, F. and Li, Z.-L.: Surface temperature and emissivity at various scales: Definition, measurement and related problems, Remote Sensing Reviews, 12, 225–253, doi:10.1080/02757259509532286, 1995.

Bosilovich, M. G.: A comparison of MODIS land surface temperature with in situ observations, Geophys. Res. Lett., 33, L20112, doi:10.1029/2006GL027519, 2006.

Bouchard, C.: Simulation du régime thermique des sols pergélisolés: essai du modèle “Tone”, Master thesis, Université Laval, 137 pp., 1990.

Coll, C., Caselles, V., Galve, J.M., Valor, E., Niclos, R., Sanchez, J. M., and Rivas, R.: Ground measurements for the validation of land surface temperatures derived from AATSR and MODIS data, Remote Sens. Environ., 97, 288–300, doi:10.1016/j.rse.2005.05.007, 2005.

Coll, C., Wan, Z., and Galve J. M.: Temperature-based and radiance- based validations of the V5 MODIS land surface temperature product, J. Geophys. Res., 114, D20102, doi:10.1029/2009JD012038, 2009.

Christensen, T. R., Johansson, T., Akerman, J. H., Mastepanov, M., Malmer, N., Friborg, T., Crill, P., and Svensson, B. H.: Thawing sub-arctic permafrost: effects on vegetation and methane emissions, Geophys. Res. Lett., 31, L04501, doi:10.1029/2003GL018680, 2004.

Comiso, J. C.: Warming trends in the Arctic from clear sky satellite observations, J. Climate, 16, 3498–3510, 2003.

Coops, N. C., Wulder, M. A., and Iwanicka D.: Large area monitoring with a MODIS-based Disturbance Index (DI) sensitive to annual and seasonal variations, Remote Sens. Environ., 113, 1250–1261, doi:10.1016/j.rse.2010.01.005, 2009.

Crosman, E. T. and Horel, J. D.: MODIS-derived surface temperature of the Great Salt Lake, Remote Sens. Environ., 113, 73–81, doi:10.1016/j.rse.2008.08.013, 2009.

Fernandes, R. A., Pavlic, G., Chen, W., and Fraser, R.: Canada-wide 1 km water fraction derived from National Topographic Data Base maps, Natural Resources Canada, Earth Science Sector, Ottawa, Ontario, Canada, http://geogratis.ca/geogratis/en/option/select.do?id=8C3D34AE-5BD5-A83C-DB8C-895FB4AD86C6, last access: 24 April 2011, 2002.






TCD
5, 1583–1625, 2011



Gahé, E.: Géomorphologie cryogène et géophysique dans la région de Kangiqsualujjuaq, Ungava, Ph.D. thesis, Université Laval, 210 pp., 1987.
Galve, J. M., Coll, C., Caselles, V., Valor, E., Niclos, R., Sanchez, J. M., and Mira, M.: Simulation and validation of land surface temperature algorithms for MODIS and AATSR data, Tethys, 4, 27–32, doi:10.3369/tethys.2007.4.04, 2007.
Gleason, A. C. R., Prince, S. D., Goetz, S. J., and Small, J.: Effects of orbital drift on land surface temperature measured by AVHRR thermal sensors, Remote Sens. Environ., 79, 147–165, PII:S0034-4257(01)00269-3, 2002.
Goïta, K. and Royer, A. B.: Surface temperature and emissivity separability over land surface from combined TIR and SWIR NOAA – AVHRR data, IEEE T. Geosci. Remote., 35, 718–733, PII:S0196-2892(97)0295-0, 1997.
Goïta, K., Royer, A. B., and Bussières, N.: Characterization of land surface thermal structure from NOAA-AVHRR data over a Northern Ecosystem, Remote Sens. Environ., 60, 282–298, PII: S0034-4257(96)00211-8, 1997.
Hachem, S., Allard, M., and Duguay, C. R.: A new permafrost map of Québec-Labrador derived from near surface temperature data of the Moderate Resolution Imaging Spectroradiometer (MODIS), in: Proceedings of the 9th International Conference on Permafrost, 1, 591–596, 2008.
Hachem, S., Allard, M., and Duguay, C.R.: Using the MODIS land surface temperature product for mapping permafrost: an application to northern Québec and Labrador, Canada, Permafrost Periglac., 20, 407–416, doi:10.1002/ppp.672, 2009.
Han, K.-S., Viau, A. A., and Anctil, F.: An Analysis of GOES and NOAA derived land surface temperatures estimated over a boreal forest, Int. J. Remote Sen., 25, 4761–4780, doi:10.1080/01431160410001680446, 2004.
Hinzman, L. D., Goering D. J., and Kane, D. L.: A distributed thermal model for calculating soil temperature profiles and depth of thaw in permafrost regions, J. Geophys. Res., 103(D22), 28975–28991, 1998.
Hinzman, L. D., Bettez, N. D., Bolton, W. R., Chapin III, F. S., Dyurgerov, M. B., Fastie, C. L., Griffith, B., Hollister, R. D., Hope, A., Huntington, H. P., Jensen, A.M., Jia, G. J., Jorgenson, T., Kane, D. L., Klein, D. R., Kofinas, G., Lynch, A. H., Lloyd, A. H., McGuire, A. D., Nelson, F. E., Oechel, W. C., Osterkamp, T. E., Racine, C. H., Romanowsky, V. E., Stone, R. S., Stow, D. A., Sturm, M., Tweedie, C. E., Vourlitis, G. L., Walker, M. D., Walker, D. A., Webber, P.J., Welker, J.M., Winker, K., and Yoshikawa K.: Evidence and implications of recent





TCD
5, 1583–1625, 2011



climate change in northern Alaska and other arctic regions, Climatic Change, 72, 251–298, doi:10.1007/s10584-005-5352-2, 2005.

Hook, S. J., Vaughan, R. G., Tonooka, H., and Schladow, S. G.: Absolute radiometric inflight validation of mid infrared and thermal infrared data from ASTER and MODIS on the Terra Spacecraft using the Lake Tahoe, CA/NV, USA, automated validation site, IEEE T. Geosci. Remote., 45, 1798–1807, doi:10.1109/TGRS.2007.894564, 2007.

Jia, G. J. and Epstein, H. E.: Controls over intra-seasonal dynamics of AVHRR NDVI for the Arctic tundra in northern Alaska, Int. J. Remote Sens., 25, 1547–1564, doi:10.1080/0143116021000023925, 2004.

Jin, M. and Treadon, R. E.: Correcting the orbit drift effect on AVHRR land surface skin temperature measurements, Int. J. Remote Sens., 24, 4543–4558, doi:10.1080/0143116031000095943, 2003.

Justice, C. O., Vermote, E., Townshend, J. R. G., Defries, R., Roy, D. P., Hall, D. K., Salomonson, V. V., Privette, J. L., Riggs, G., Strahler, A., Lucht, W., Myneni, R. B., Knyazikhin, Y., Running, S. W., Nemani, R. R., Wan, Z., Huete, A. R., Leeuwen, W. V., Wolfe, R. E., Giglio, L., Muller, J.-P., Lewis, P., and Barnsley, M. J.: The Moderate Resolution Imaging Spectroradiometer (MODIS): Land Remote Sensing for Global Change Research, IEEE T. Geosci. Remote., 36, 1228–1249, PII: S0196-2892(98)04751-2, 1998.

Kerr, Y. H., Lagouarde, J. P., and Imbernon, J.: Accurate land surface temperature retrieval from AVHRR data with use of an improved split window algorithm, Remote Sens. Environ., 41, 197–209, 1992.

Kheyrollah Pour, H., Duguay, C. R., Martynov, A., and Brown, L. C.: Simulation of surface temperature and ice cover of large northern lakes with 1-D models: A comparison with MODIS satellite data and in situ measurements, Tellus A, in review, 2011.

Kohn, J. and Royer, A.: AMSR-E data inversion for soil temperature estimation under snow cover, Remote Sens. Environ., 114, 2951–2961, doi:10.1016/j.rse.2010.08.002, 2010.

Langer, M., Westermann, S., and Boike, J.: Spatial and temporal variations of summer surface temperatures of wet polygonal tundra in Siberia – implications for MODIS LST based permafrost monitoring, Remote Sens. Environ., 114, 2059–2069, doi:10.1016/j.rse.2010.04.012, 2010.

Li, Z.-L. and Becker, F.: Feasibility of land surface temperature and emissivity determination from AVHRR data, Remote Sens. Environ., 43, 67–85, 1993.





Mialon, A., Royer, A., Fily, M., and Picard, G.: Daily microwave-derived surface temperature over Canada/Alaska, J. Appl. Meteorol. Clim., 46, 591–604, doi:10.1175/JAM2485.1, 2007.
Meunier, C., Sirois, L., and Bégin, Y.: Climate and Picea Mariana seed maturation relationships: a multi-scale perspective, Ecol. Monogr., 77, 361–376, doi:10.1890/06-1543.1, 2007.
Ouaidrari, H., Goward, S. N., Czajkowski, K. P., Sobrino, J. A., and Vermote, E.: Land surface temperature estimation from AVHRR thermal infrared measurements, An assessment for the AVHRR Land Pathfinder II data set, Remote Sens. Environ., 81, 114–128, PII: S0034-4257(01)00338-8, 2002.
Royer, A. and Poirier, S.: Surface temperature spatial and temporal variations in North America from homogenized satellite SMMR – SSM/I microwave measurements and reanalysis for 1979–2008, J. Geophys. Res.-Atmos, 115, D08110, doi:10.1029/2009JD012760, 2010.
Sazonova, T. and Romanovsky, V. E.: A model for regional scale estimation of temporal and spatial variability of active layer thickness and mean annual ground temperatures, Permafrost Periglac., 14, 125–139, doi:10.1002/ppp.449, 2003.
Schubert, P., Eklundh, L., Lund, M., and Nilsson, M.: Estimations northern peatland $CO_2$ exchange from MODIS time series data, Remote Sens. Environ., 114, 1178–1189, doi:10.1175/JAM2485.1, 2010.
Serreze, M. C., Walsh, J. E., Chapin III, F. S., Osterkamp, T. E., Dyurgerov, M. B., Romanovsky, V. E., Oechel, W. C., Morison, J., Zhang, T., and Barry, R. G.: The observational evidence of recent change in the northern high latitude environment, Climatic Change, 46, 159–207, doi:10.1023/A:1005504031923, 2000.
Shiklomanov, N. I. and Nelson, F. E.: Active-layer mapping at regional scales: a 13-Year spatial time series for the Kuparuk Region, North-Central Alaska, Permafrost Periglac., 13, 219–230, doi:10.1002/ppp.425, 2002.
Shiklomanov, N. I., Anisimov, O. A., Zhang, T., Marchenko, S., Nelson, F. E., and Oelke, C.: Comparison of model-produced active layer fields: results for northern Alaska, J. Geophys. Res., 112, F02S10, doi:10.1029/2006JF000571, 2007.
Snyder, W.C., Wan, Z., Zhang, Y., and Feng, Y.-Z.: Requirements for satellite land surface temperature validation using a Silt Playa, Remote Sens. Environ., 6, 279–289, 1997.
Snyder, W. C., Wan, Z., Zhang, Y., and Feng, Y.-Z.: Classification-based emissivity for land surface temperature measurement from space, Int. J. Remote Sens., 19, 2753–2774, doi:10.1080/014311698214497, 1998.





TCD
5, 1583–1625, 2011



Traoré, P. C. S., Royer, A. B., and Goïta, K.: Land surface temperature time series derived from weekly AVHRR GVI composite datasets: Potential and constraints for Northern Latitudes, Can. J. Remote Sens., 4, 390–400, 1997.

Wan, Z.: MODIS Land Surface Temperature products user's guide. Institute for Computational Earth System Science, University of California, Santa Barbara, CA, http://www.icess.ucsb.edu/modis/LstUsrGuide/MODIS_LST_products_Users_guide_C5.pdf, last access: 27 April 2011, 2007.

Wan, Z.: New refinements and validation of the MODIS land-surface temperature/emissivity products, Remote Sens. Environ., 112, 59–74, doi:10.1016/j.rse.2006.06.026, 2008.

Wan, Z. and Dozier, J.: Land surface temperature measurement from space: physical principles and inverse modeling, IEEE T. Geosci. Remote., 27(3), 268–278, doi:10.1109/36.17668, 1989.

Wan, Z. and Dozier, J.: A generalized split-window algorithm for retrieving land-surface temperature from space, IEEE T. Geosci. Remote., 34, 892–905, doi:10.1109/36.508406, 1996.

Wan, Z. and Li, Z.-L.: A physics-based algorithm for retrieving land-surface emissivity and temperature from EOS/MODIS data, IEEE T. Geosci. Remote., 35, 980–996, doi:10.1109/36602541, 1997.

Wan, Z. and Li, Z-L.: Radiance-based validation of the V5 MODIS land-surface temperature product, Int. J. Remote Sens., 29, 5373–5395, doi:10.1080/01431160802036565, 2008.

Wan, Z., Zhang, Y., Li, Z.-L., Wang, R., Salomonson, V. V., Yves, A., Bosseno, R., and Hanocq, J. F.: Preliminary estimate of calibration of the Moderate Resolution Imaging Spectroradiometer thermal infrared data using Lake Titicaca, Remote Sens. Environ., 80, 497–515, PII: S0034-4257(01)00327-3, 2002a.

Wan, Z., Zhang, Y., Zhang, Q., and Li Z.-L.: Validation of the land-surface temperature products retrieved from Terra Moderate Resolution Imaging Spectroradiometer data, Remote Sens. Environ., 83, 163–180, PII:S0034-4257(02)00093-7, 2002b.

Wan, Z., Zhang, Y., Zhang, Q., and Li Z.-L.: Quality assessment and validation of the MODIS global land surface temperature, Int. J. Remote Sens., 25, 261–274, doi:10.1080/0143116031000116417, 2004.

Westermann, S., Langer, M., and Boike, J.: Spatial and temporal variations of summer surface temperatures of high-arctic tundra on Svalbard — Implications for MODIS LST based permafrost monitoring, Remote Sens. Environ., 115, 908–922, doi:10.1016/j.rse.2010.11.018, 2011.





TCD
5, 1583–1625, 2011



Williams, P. J. and Smith, M. W.: The frozen earth: fundamentals of geocryology. Cambridge: Cambridge University Press, 306 pp., 1989.

Zhou, L., Tucker, C. J., Kaufmann, R. K., Slayback, D. A., Shabanov, N. V., and Myneni, R. B.: Variations in northern vegetation activity inferred from satellite data of vegetation index during 1981 to 1999, J. Geophys. Res.-Atmos, 106, (D17), 20069–20083, 2001.





TCD

5, 1583–1625, 2011



**Table 1.** Characteristics of the study sites.

| Station Name | Station coordinates | | Height Tair (m) | Depth Tsol(cm) | Elevation(m) | Vegetation cover | Soil Characteristics |
|---|---|---|---|---|---|---|---|
| | Latitude (N) | Longitude (W) | /frequency of measurements hourly | /frequency of measurements: * | | | |
| *Alaska* | | | | | | | |
| West Dock (WD) | 70°22′ 50″ | 148°33′ 39″ | 1 | - | 7–6 | Marshy drained lake basin tundra | Organic overlying layers of fine sans and silts |
| Betty Pingo wetland (BPW) | | | 1 | Surface/h | | Wet sedge tundra and furb tundra | |
| Betty Pingo upland (BPU) | 70°16′46.3” | 148° 53′ 44.5″ | – | Surface/h | 12 | Marshy drier more tundra | Organic overlying layers of fine sand and silts |
| Franklin Bluff (FB) | 69°53′ 31.8″ | 148°46′ 4.8″ | 1 | Surface/h | 78 | Grasses and sedges rooted in mosses and lichens | Organic materials of variable thickness overlie silt loam textured mineral soils poorly drained |
| Sagwon (SAG) | 69°25′ 27.5″ | 148°41′ 45.1″ | 1 | Surface/d | 299 | Tussock tundra | Loamy with peaty surface layer poorly drained |
| West Kuparuk (WK) | 69°25′ 34.3″ | 150°20′ 25.3″ | 1 | 2/d | 158 | Moist acidic tundra, tussock tundra | Loamy with peaty surface layer poorly drained |
| Upper Kuparuk (UK) | 68°38′ 24.5” | 149°24′ 23.4” | 1 | 5/d | 774 | Tussock tundra | – |
| Imnavait Basin (IB) | 68°36′ 58.6″ | 149°18′ 13.0″ | 1 | Surface/d | 937 | Tussock tundra mosses lichens shrubs | Soils cold wet poorly draned sil loams with a high organic content and include many glacial erratic |
| Imnavait Ridge (IR) | 68°37′ 27.9″ | 149°19′ 22.3″ | – | Surface/d | – | – | – |
| Ivotuk Shrub (IvShrb) | 68°29′ 12″ | 155°44′ 34″ | 1 | 2.5/3 h | 570 | Shrub lichen tussock | – |
| Ivotuk Moss (Iv-Moss) | 68°26′ 58.6″ | 155°44′ 71′ | 1 | 1/3 h | | Moss lichen tussock | – |
| *Québec* | | | | | | | |
| Sila | 62°11′ 41.9″ | 75°38′ 12.8″ | 2 | 3/h | 45 | Moss lichen tussock | Organic overlying very shallow thickness of silt on till |
| Tiki | 62°12′ 14.1″ | 75°41′ 11.6″ | 2 | 3/h | 35 | lichen | Bed rock, nor organic matter |
| Salluit airport (SalA) | 62°11′ 1.44″ | 75°39′54.9″ | 2 | – | – | – | Rock, asphalt |
| Kangiqsuallujjuaq (Kangiq) | 58°41′ 7.83″ | 65°55′ 6.43″ | 2 | 3/h | 110 | Lichen and shrub of birch | Organic overlying shallow till on bed rock |
| Kuujjuaq (Env. Can.) | 58°06′ 31.62″ | 68°24′ 42.44″ | 1.5 | – | 39 | – | – |

*h : measured each hour; d : mean daily temperature; - No Data





TCD
5, 1583–1625, 2011



**Table 2.** Correspondence between stations and MODIS pixels used for comparison.

| Station Name | | Time period of station measurements | Pixel Name | Pixel center coordinate Latitude (N) | Longitude (W) | MODIS tile | Pixel position description |
|---|---|---|---|---|---|---|---|
| *Alaska* | | | | | | | |
| West Dock | Tair: | 03/02/2000 to 29/10/2008 | WD1<br>WD2 | 70°22′ 50″<br>70° 22′ 20.33″ | 148° 33′ 39″<br>148°34′ 16.24″ | h13v01<br>h13v01 | Near the coast (57.5 % water)<br>One pixel south of WD1 (28.1 % water) |
| Betty Bingo (upland) – Tsoil<br>Betty Pingo (wetland) – Tair | Tsoil:<br>Tair: | 01/01/2000 to 19/10/2008<br>01/01/2000 to 31/12/2008 | BPU1<br>BPW1 | 70°16′ 46.3″<br>70°16′46.7″ | 148°53′ 44.5″<br>148°53′46″ | h12v01<br>h12v01 | One pixel of water (1.5 % water), same pixel kept<br>Twelve pixels of water (17.9 % water), same pixel kept |
| Eastern Kuparuk (Franklin Bluff) | Tair:<br>Tsoil: | 01/01/2000 to31/12/2007<br>29/04/2001 to 31/12/2007 | FB1<br>FB2 | 69°53′31.8″<br>69°53′27.12″ | 148°46′4.8″<br>148°46′59.95″ | h12v02<br>h12v02 | Close to a river (60 % of wet graminoid)<br>One pixel east of FrB1 (50 % of wet graminoid) |
| Eastern Kuparuk (Sagwon) | Tair:<br>Tsoil: | 01/01/2000 to 31/12/2008<br>01/01/2003 to 28/12/2008 | SAG1 | 69°25′ 27.5″ | 148°41′ 45.1″ | h12v02 | No water, same pixel kept |
| West Kuparuk | Tair:<br>Tsoil: | 25/04/2000 to 22/09/2008<br>25/04/2000 to 16/09/2008 | WK1<br>WK2 | 69°25′34.3″<br>69°26′09.62″ | 150°20′25.3″<br>150°19′47.70″ | h12v02<br>h12v02 | No water, same pixel kept<br>One pixel north west of WK1 (7.2 % water) |
| Upper Kuparuk | Tair: | 01/03/2000 to 14/09/2008 | UK1 | 68°38′24.56″ | 149°24′23.4″ | h12v02 | One pixel of water (2 % water), same pixel kept |
| Imnavait Basin | Tair:<br>Tsoil: | 01/01/2000 to 31/12/2008<br>01/01/2000 to 25/10/2007 | IB1<br>IB2 | 68°36′ 58.6″<br>68°37′ 2.7″ | 149°18′ 13″<br>149°19′ 2.3″ | h12v02<br>h12v02 | No water, same pixel kept<br>One pixel north west of IB1 (no water) |
| Ivotuk Shrub | Tair: | 01/01/2000 to 31/12/2004 | IvShrb1 | 68°29′ 12″ | 155°44′ 34″ | h12v02 | No water, same pixel kept |
| Ivotuk Moss | Tair: | 01/01/2000 to 31/12/2004 | IvMoss1 | 68°28′ 49.2″ | 150°44′42.6″ | h12v02 | No water, same pixel kept |
| *Québec* | | | | | | | |
| Sila | Tair / Tsoil | 05/08/2002 to 13/10/2003 | Sila1 | 62°11′ 41.9″ | 75°38′ 12.8″ | h14v02 | Near the coast (9.7 % water), same pixel kept |
| Tiki | Tair/Tsoil | 30/07/2002 to 13/10/2003 | Tiki1<br>Tiki2 | 62°12′ 14.1″ | 75°41′ 11.6″ | h14v02<br>h14v02 | In the water (100 % water)<br>One pixel south of Tiki (17.5 % water) |
| Salluit airport | Tair: | 28/07/2002 to 14/10/2007 | SalA1 | 62°11′ 1.44″ | 75°39′ 54.9″ | h14v02 | No water, same pixel kept |
| Kangiqsuallujjuaq | Tair: | 05/06/2001 to 02/11/2004 | Kangiq1<br>Kangiq2 | 58°41′ 28.2″ | 65°55′ 23.16″ | h14v03<br>h14v03 | Near the coast (10.4 % water)<br>One pixel right (8.9 % water) |
| Kuujjuaq | Tair: | 01/01/2000 to 31/12/2008 | Kuujjuaq1<br>Kuujjuaq2<br>Kuujjuaq3 | 58°06′ 31.62″ | 68°24′ 42.44″ | h14v03<br>h14v03<br>h14v03 | This pixel containing the station had no LST values:<br>One pixel right and one down (no water)<br>One pixel left (no water) |

1:pixel including station; 2 or 3: other pixel





TCD
5, 1583–1625, 2011



**Table 3.** Number of days (percentage) with clear-sky MODIS LST measurements (2000–2008).

| Pixel Name | 2000 | 2001 | 2002 | 2003 | 2004 | 2005 | 2006 | 2007 | 2008 |
|---|---|---|---|---|---|---|---|---|---|
| *Alaska* | | | | | | | | | |
| WD1 | – | – | 26 % | 33 % | 40 % | 36 % | 31 % | 38 % | 36 % |
| WD2 | – | – | 29 % | 34 % | 41 % | 39 % | 32 % | 36 % | 36 % |
| BPW1 | 23 % | 24 % | 37 % | 41 % | 54 % | 50 % | 47 % | 49 % | 44 % |
| FB1 | 27 % | 24 % | 39 % | 40 % | 52 % | 40 % | 43 % | 53 % | 41 % |
| FB2 | 27 % | 27 % | 39 % | 42 % | 53 % | 39 % | 43 % | 54 % | 40 % |
| SAG1 | 26 % | 31 % | 42 % | 44 % | 53 % | 48 % | 45 % | 58 % | 41 % |
| WK1 | 27 % | 28 % | 38 % | 43 % | 53 % | 43 % | 44 % | 56 % | 43 % |
| WK2 | 26 % | 29 % | 39 % | 45 % | 53 % | 43 % | 46 % | 56 % | 44 % |
| UK1 | 31 % | 32 % | 38 % | 46 % | 53 % | 51 % | 47 % | 58 % | 48 % |
| IB1 | 32 % | 32 % | 35 % | 45 % | 54 % | 54 % | 43 % | 59 % | 48 % |
| IB2 | 33 % | 33 % | 37 % | 46 % | 53 % | 53 % | 45 % | 61 % | 48 % |
| IvMoss | 25 % | 27 % | 41 % | 44 % | 63 % | 65 % | 54 % | 69 % | 60 % |
| IvShrb | 25 % | 27 % | 42 % | 44 % | 50 % | 51 % | 41 % | 55 % | 44 % |
| *Québec* | | | | | | | | | |
| Sila1 | – | – | 15 % | 18 % | 17 % | 17 % | 19 % | 19 % | 21 % |
| Tiki2 | – | – | 15 % | 18 % | 18 % | 18 % | 22 % | 21 % | 22 % |
| SalA1 | – | – | 17 % | 19 % | 18 % | 16 % | 22 % | 21 % | 23 % |
| Kangiq1 | – | 16 % | 14 % | 17 % | 19 % | 22 % | 20 % | 16 % | 26 % |
| Kangiq2 | – | 16 % | 16 % | 17 % | 18 % | 21 % | 19 % | 14 % | 24 % |
| Kujjuaq2 | 10 % | 19 % | 21 % | 30 % | 28 % | 33 % | 33 % | 28 % | 40 % |
| Kujjuaq3 | 5 % | 9 % | 13 % | 16 % | 14 % | 15 % | 15 % | 14 % | 18 % |





TCD
5, 1583–1625, 2011



**Table 4.** Frequency of Aqua and Terra satellite overpasses within different hours above the field stations during the period of study (2000–2008). The most frequent overpass times for the different stations are given in bold.

| | Aqua overpass hours | | | | | | | | | | | | Terra overpass hours | | | | | | | | | | | |
|---|---|---|---|---|---|---|---|---|---|---|---|---|---|---|---|---|---|---|---|---|---|---|---|---|
| | Day Time | | | | | | Night time | | | | | | Day time | | | | | | Night time | | | | | |
| Pixels Over Alaska | **9** | **10** | **11** | **12** | **13** | **14** | **0** | **1** | **2** | **3** | **4** | **5** | **10** | **11** | **12** | **13** | **14** | **15** | **18** | **19** | **20** | **21** | **22** | **23** |
| WD1 | 0.13 | 0.25 | 0.21 | **0.26** | 0.10 | 0.05 | 0.13 | **0.35** | 0.18 | 0.19 | 0.11 | 0.05 | 0.07 | **0.29** | 0.25 | 0.11 | 0.10 | 0.18 | 0.09 | 0.25 | **0.28** | **0.28** | 0.09 | 0.02 |
| WD2 | 0.13 | 0.25 | 0.22 | **0.27** | 0.09 | 0.05 | 0.13 | **0.34** | 0.18 | 0.18 | 0.12 | 0.04 | 0.07 | **0.28** | 0.26 | 0.11 | 0.09 | 0.17 | 0.09 | 0.25 | **0.29** | 0.28 | 0.08 | 0.02 |
| BPU1 | 0.13 | **0.30** | 0.20 | 0.21 | 0.11 | 0.04 | 0.14 | **0.36** | 0.17 | 0.18 | 0.11 | 0.04 | 0.07 | **0.27** | 0.23 | 0.10 | 0.13 | 0.18 | 0.10 | 0.25 | **0.29** | 0.27 | 0.08 | 0.01 |
| BPW1 | 0.13 | **0.30** | 0.20 | 0.21 | 0.11 | 0.04 | 0.14 | **0.36** | 0.18 | 0.18 | 0.10 | 0.04 | 0.07 | **0.27** | 0.23 | 0.10 | 0.13 | 0.19 | 0.10 | 0.25 | **0.29** | 0.27 | 0.08 | 0.01 |
| FB1 | 0.10 | **0.28** | 0.23 | 0.25 | 0.10 | 0.03 | 0.17 | **0.38** | 0.17 | 0.16 | 0.08 | 0.03 | 0.06 | **0.32** | 0.24 | 0.11 | 0.13 | 0.14 | 0.08 | 0.26 | **0.27** | 0.26 | 0.11 | 0.02 |
| FB2 | 0.10 | **0.30** | 0.22 | 0.23 | 0.11 | 0.04 | 0.16 | **0.37** | 0.17 | 0.17 | 0.10 | 0.04 | 0.06 | **0.33** | 0.22 | 0.09 | 0.14 | 0.15 | 0.08 | 0.26 | **0.28** | 0.26 | 0.10 | 0.02 |
| SAG1 | 0.06 | **0.30** | 0.29 | 0.22 | 0.09 | 0.04 | 0.18 | **0.39** | 0.16 | 0.15 | 0.08 | 0.03 | 0.07 | **0.35** | 0.24 | 0.10 | 0.13 | 0.11 | 0.05 | 0.29 | **0.30** | 0.25 | 0.10 | 0.02 |
| WK1 | 0.06 | **0.29** | 0.28 | 0.20 | 0.10 | 0.06 | 0.19 | **0.40** | 0.15 | 0.15 | 0.07 | 0.03 | 0.07 | **0.35** | 0.20 | 0.10 | 0.17 | 0.12 | 0.06 | **0.30** | **0.30** | 0.24 | 0.09 | 0.01 |
| WK2 | 0.07 | **0.29** | 0.27 | 0.21 | 0.11 | 0.06 | 0.18 | **0.40** | 0.15 | 0.16 | 0.07 | 0.04 | 0.07 | **0.35** | 0.20 | 0.09 | 0.16 | 0.12 | 0.06 | **0.31** | 0.29 | 0.24 | 0.09 | 0.01 |
| UK1 | – | 0.30 | **0.35** | 0.22 | 0.09 | 0.04 | 0.18 | **0.41** | 0.15 | 0.16 | 0.08 | 0.02 | 0.11 | **0.44** | 0.23 | 0.08 | 0.11 | 0.03 | – | 0.27 | **0.36** | 0.26 | 0.10 | 0.02 |
| IB1 | – | 0.30 | **0.36** | 0.21 | 0.10 | 0.02 | 0.17 | **0.41** | 0.16 | 0.16 | 0.08 | 0.02 | 0.10 | **0.44** | 0.23 | 0.08 | 0.12 | 0.03 | – | 0.27 | **0.37** | 0.25 | 0.09 | 0.02 |
| IB2 | – | 0.31 | **0.37** | 0.20 | 0.10 | 0.02 | 0.16 | **0.40** | 0.17 | 0.16 | 0.08 | 0.02 | 0.10 | **0.43** | 0.25 | 0.09 | 0.11 | 0.03 | – | 0.26 | **0.37** | 0.26 | 0.09 | 0.02 |
| IvShrb1 | – | 0.25 | **0.29** | 0.20 | 0.11 | 0.15 | 0.18 | **0.40** | 0.16 | 0.16 | 0.07 | 0.03 | 0.09 | **0.34** | 0.24 | 0.08 | 0.22 | 0.03 | – | 0.22 | **0.34** | 0.29 | 0.12 | 0.03 |
| IvMoss1 | – | 0.25 | **0.30** | 0.20 | 0.10 | 0.15 | 0.18 | **0.41** | 0.16 | 0.16 | 0.06 | 0.03 | 0.08 | **0.34** | 0.24 | 0.08 | 0.23 | 0.03 | – | 0.21 | **0.34** | 0.31 | 0.12 | 0.02 |
| Pixels Over Québec | **9** | **10** | **11** | **12** | **13** | **14** | **0** | **1** | **2** | **3** | **4** | **5** | **10** | **11** | **12** | **13** | **14** | **15** | **18** | **19** | **20** | **21** | **22** | **23** |
| Sila1 | – | – | 0.19 | **0.40** | 0.36 | 0.06 | 0.09 | 0.16 | 0.28 | **0.40** | 0.07 | – | 0.07 | **0.41** | 0.41 | 0.12 | – | – | – | – | 0.15 | **0.47** | 0.33 | 0.05 |
| Tiki2 | – | – | 0.18 | 0.38 | **0.39** | 0.06 | 0.09 | 0.15 | 0.29 | **0.38** | 0.08 | – | 0.06 | **0.41** | 0.40 | 0.13 | – | – | – | – | 0.15 | **0.45** | 0.34 | 0.06 |
| SalA1 | – | – | 0.18 | **0.49** | 0.37 | 0.06 | 0.05 | 0.12 | 0.36 | **0.38** | 0.09 | – | 0.07 | **0.41** | 0.39 | 0.12 | – | – | – | – | 0.15 | **0.46** | 0.34 | 0.06 |
| Kangiq1 | – | – | 0.07 | 0.38 | **0.43** | 0.12 | 0.07 | 0.12 | 0.35 | **0.37** | 0.08 | – | 0.09 | **0.44** | 0.37 | 0.10 | – | – | – | – | 0.09 | **0.45** | 0.38 | 0.08 |
| Kangiq2 | – | – | 0.08 | 0.38 | **0.43** | 0.11 | 0.07 | 0.13 | **0.37** | 0.35 | 0.07 | – | 0.09 | **0.44** | 0.37 | 0.10 | – | – | – | – | 0.10 | **0.44** | 0.38 | 0.08 |
| Kujjuaq2 | – | – | 0.06 | 0.38 | **0.47** | 0.09 | 0.10 | 0.19 | **0.36** | 0.28 | 0.07 | – | 0.08 | **0.49** | 0.36 | 0.07 | – | – | – | – | 0.11 | **0.44** | 0.36 | 0.09 |
| Kujjuaq3 | – | – | 0.05 | 0.37 | **0.48** | 0.10 | 0.07 | 0.16 | **0.41** | 0.31 | 0.05 | – | 0.09 | **0.48** | 0.35 | 0.07 | – | – | – | – | 0.11 | **0.46** | 0.34 | 0.09 |





TCD
5, 1583–1625, 2011



**Table 5.** Mean difference and correlation for daytime, nighttime and daily average from Aqua and Terra separately, and Aqua/Terra combined.

| | | | Daytime mean | Nighttime mean | Daily mean |
|---|---|---|---|---|---|
| Alaska (Ak) | Terra | Mean difference | −0.70 | −2.87 | −1.37 |
| | | *R* | 0.96 | 0.94 | 0.97 |
| | Aqua | Mean difference | −1.21 | −4.57 | −2.69 |
| | | *R* | 0.97 | 0.96 | 0.98 |
| | Terra/Aqua | Mean difference | −0.98 | −3.48 | −1.90 |
| | | *R* | 0.97 | 0.96 | 0.98 |
| Québec (Qc) | Terra | Mean difference | 0.39 | −5.43 | −1.72 |
| | | *R* | 0.96 | 0.91 | 0.95 |
| | Aqua | Mean difference | 1.12 | −6.11 | −1.28 |
| | | *R* | 0.95 | 0.93 | 0.96 |
| | Terra/Aqua | Mean difference | 0.41 | −5.93 | −1.79 |
| | | *R* | 0.96 | 0.91 | 0.96 |
| Ak and Qc | Terra/Aqua | Mean difference | −0.54 | −4.26 | −1.86 |
| | | *R* | 0.96 | 0.94 | 0.97 |





TCD
5, 1583–1625, 2011



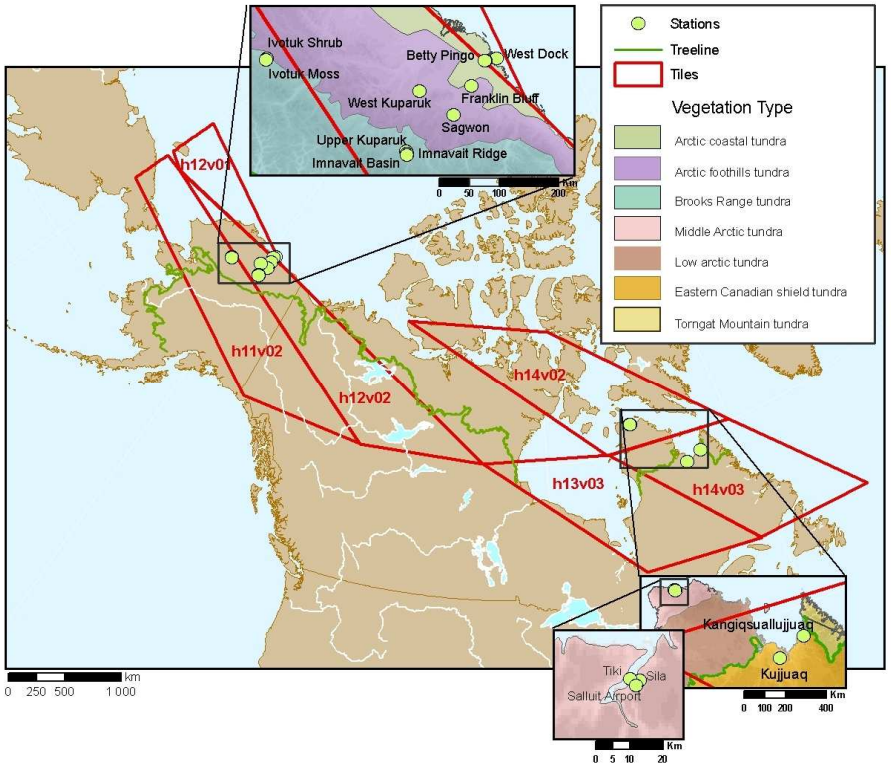


**Fig. 1.** Location of field sites and MODIS tiles for the North Slope of Alaska and Nunavik (Québec) in a Lambert conic conformal projection.





TCD
5, 1583–1625, 2011



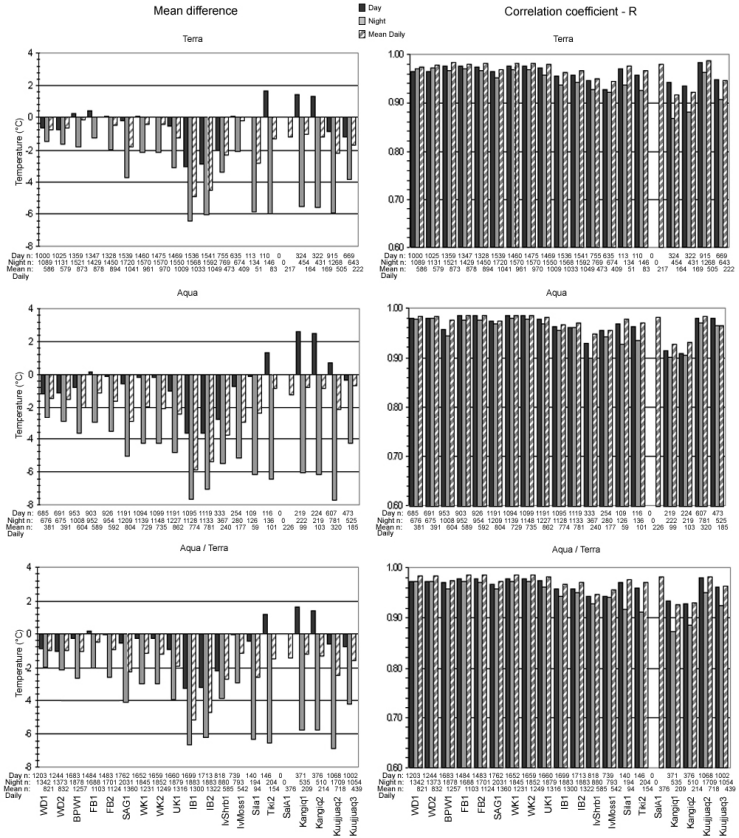


**Fig. 2.** Mean difference and correlation between $T_{air}$ and LST from Aqua, Terra and average Aqua/Terra, for day, night and mean daily values ($n$: number of measurements).





TCD
5, 1583–1625, 2011



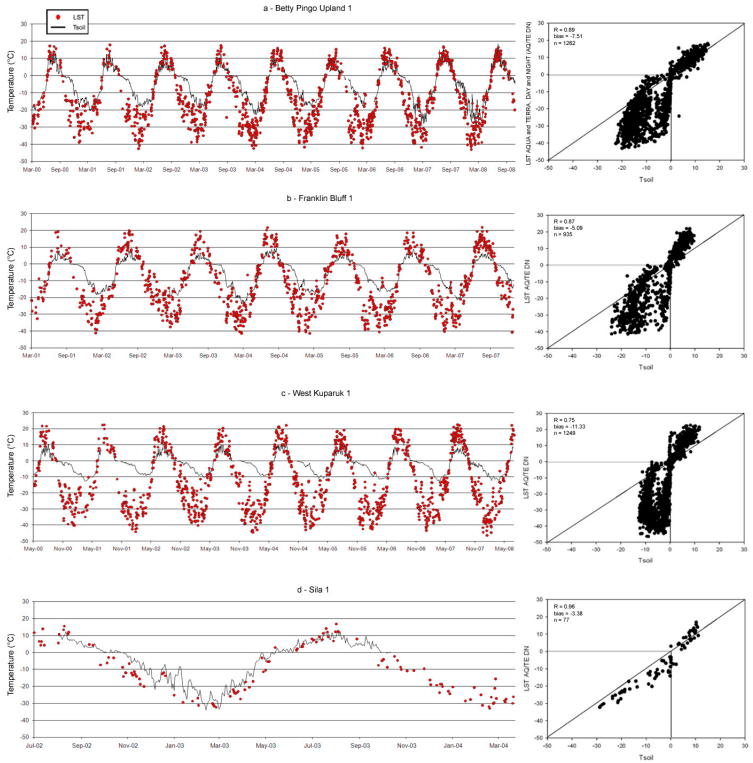


**Fig. 3.** Relation between mean daily MODIS LST (combined Terra and Aqua) and mean daily soil temperature at **(a)** Betty Pingo Upland (BPU1), **(b)** Franklin Bluff (FB1), **(c)** Western Kuparuk (WK1), and **(d)** Sila (Sila1).





TCD
5, 1583–1625, 2011



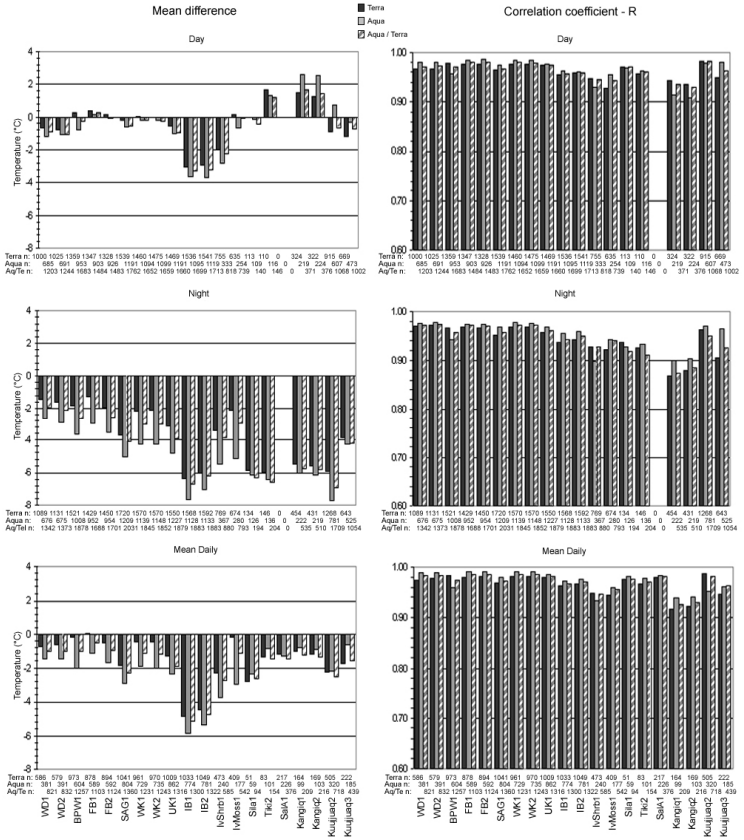


**Fig. 4.** Mean difference and correlation between $T_{air}$ and LST at daytime, nighttime, and daily average for Terra, Aqua and Aqua/Terra combined.





TCD
5, 1583–1625, 2011



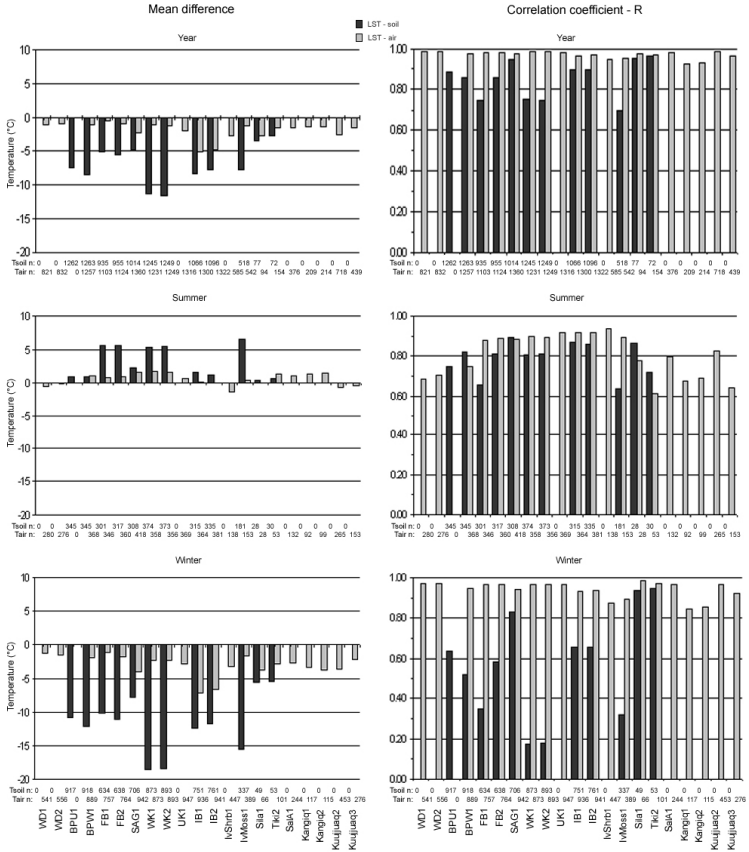


**Fig. 5.** Mean difference and correlation between daily average $T_{soil}/T_{air}$ and LST calculated from Aqua/Terra combined for full year, summer and winter periods.





TCD
5, 1583–1625, 2011

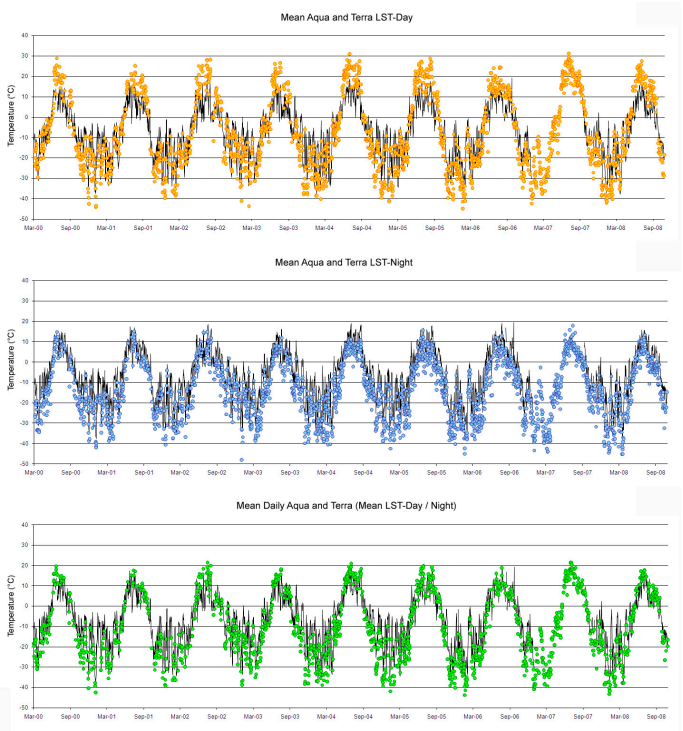


**Fig. 6.** Comparison between the mean LST **(a)** combined Terra/Aqua Day acquisitions, **(b)** combined Terra/Aqua Night acquisitions, and (c) combined Terra/Aqua Day/Night acquisitions for IB1 pixel on Imnavait Basin site.





TCD
5, 1583–1625, 2011



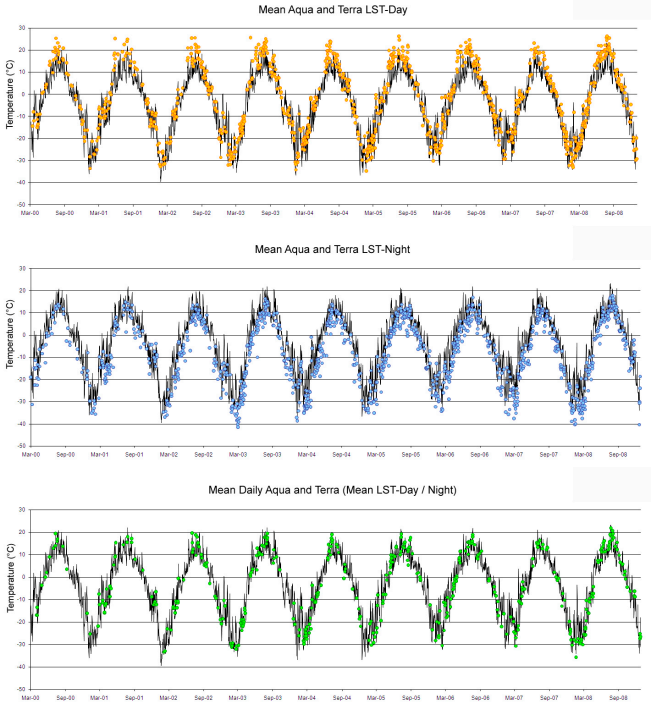


**Fig. 7.** Comparison between the mean LST **(a)** combined Terra/Aqua Day acquisitions, **(b)** combined Terra/Aqua Night acquisitions, and **(c)** combined Terra/Aqua Day/Night acquisitions for Kuujjuaq2 on Kuujjuaq site.





TCD
5, 1583–1625, 2011



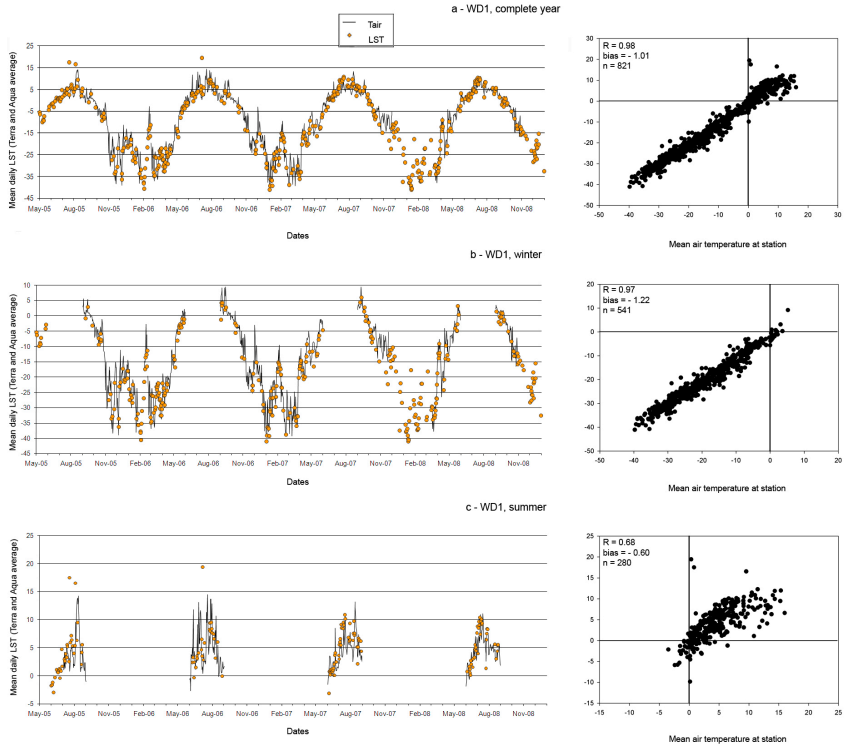


**Fig. 8.** Comparison between the mean daily LST (combined Day/Night/Terra/Aqua) and mean daily air temperature at West Dock (WD1) for **(a)** complete year, **(b)** winter, and **(c)** summer. On left, LST overlayed on meteorological station measurements, and on right relation between the two sets of measurements.





TCD
5, 1583–1625, 2011